Quantification of fragmentation capture materials and an assessment of the viability of economical alternatives: a preliminary study

James Read[1], Thomas Ritchie[1], Laura Brown[1], Susie Bloodworth-Race[1], Bonny Thawani[1], Rachael Hazael[1]* and Richard Critchley[1*],

[1] Cranfield Forensic Institute, Cranfield University, Defence Academy of the United Kingdom, Shrivenham, SN6 8LA, United Kingdom

*Corresponding Author: Rachael.Hazael@Cranfield.ac.uk and R.critchley@cranfield.ac.uk

Key Words

Abstract

High pressure, high temperature events need to be quantified experimentally. Where fragmentation occurs i.e. against Personal Protective Equipment (PPE), there is a requirement for both a reliable and repeatable measurement of numerous experimental metrics. Typically, the most critical is calculating the energy absorbed by the target material, to characterise target performance. This is achieved by detonating a device and capturing a proportion of the fragmentation in a suitable material that can achieve successful recovery of all fragmentation produced. Therefore, allowing the estimation of the target's response using the depth of penetration within the capture material which allows the calculation of energy absorption.

The current standardised fragmentation capture material used within the United Kingdom is known as strawboard. Although effective, this material is both expensive and limited in its availability. This study explores the classification of strawboard to provide a suitable baseline to compare against Medium Density Fibreboard (MDF) and flooring underlay which represent two more economically friendly alternatives on the open market. It was found that the uniformity of response for the MDF material was better than that of strawboard, due to its reproducibility between batches and velocity ranges. To further explore this phenomena, high explosive trials were conducted, further demonstrating MDF to be a viable, reliable, and cheaper alternative.

1 Introduction

Existing literature suggests there are three main reasons for studying fragmentation with many of these areas requiring examination within a single experimental series (1-4). These areas are to examine the dispersion of fragmentation propelled using blast waves generated from the explosive detonation process, to carry out further testing of the fragments, and finally to measure what the fragment can do against a target e.g. Building Structure, Vehicle or PPE, which may require the measurement of fragment velocity or fragment penetration (5-6). There are a plethora of factors of

interest when studying fragmentation such as: the quantity (6-7), size of fragmentation (6, 8-11), shape of fragment (12-15), fragment material (16-22), velocity (6, 23-28), energy (26, 28-29), dispersion (5-6, 30-34), lethality (28,34-35), and penetration (36-37). These can all be of interest when the classification of fragmentation is considered. The data that can be collected is a result of the method of fragmentation capture used.

Although the original work for calculation of fragment strike velocity from penetration into strawboard witness packs was completed in the 1970s (37), at the time of writing, strawboard remains the current standard fragmentation capture material within the UK and is referenced as such in the NATO International Testing Operating Procedure (ITOP) 4-2-813 (6). The reasons for strawboard being originally selected for use as the UK standard fragment capture material are not documented. The UK Ministry of Defence (MOD) currently records the standards to which materials are made in Defence Standards (DEF STANs). To ascertain why strawboard was adopted as a standard capture material, the original Def Spec referenced by McMahon (37) was examined.

This examination revealed that strawboard is named as such only in academic literature[1], and the International Test Operations Procedure (ITOP) (6,37). Examination of the current DEF STANs (16,22,26,28) highlighted that the only material that could be interpreted as being strawboard is Orientated Strand Board/Orientated Straw Board (OSB). DEF STAN 93-59 describes a material that is also called chipboard (26), and that this is for use at Proofing and Testing Establishments. However, the exact same material, named millboard (38), is for use as an ammunition packing material. The adoption of millboard as the standard fragmentation capture material (referred to as chipboard) required the additional quality assurance requirement of testing the bursting strength. The assumption is that millboard was adopted as chipboard for use at Proofing and Experimental Establishments. The reason for the academic name for chipboard becoming strawboard remains unknown. For clarity, the chipboard/millboard/strawboard material will be referred to as strawboard throughout this study.

It is speculated that strawboard was a material of convenience rather than being a designed standard. The only additional quality assurance regime consisted of a burst strength test which gave the material a known parameter for quality assurance. This parameter was measured using a Mullen Test, this is a measure of the total hydraulic pressure expanding a diaphragm. When the sample ruptures this pressure value is its bursting strength. This process is repeated on both sides of the material and thus is expressed as the average of both sides. A comparison of the Def Spec 81/001 (16) to the DEFSTAN 93-59 (26) is in Table 1. Due to the change in standard units the Def Spec shows the original values and conversions to current units of measure in brackets. This reveals that the standard capture material tolerances for thickness, grammage and busting strength have changed slightly in the last 50 years.

Table 1 - Comparison of manufacturing standards for strawboard from Def Spec 81/001 (16) and DEFSTAN 93-59 (26).

Document	Thickness Range	Grammage Range	Bursting Strength
Def Spec 81/001	3.45 – 3.75 mm (Average 3.60 mm)	2650 – 2780 g/m^2 (1.29 – 1.36 cm^3/g)	Min 330 lb/sq in (Min 2275 KPa)

---

[1] The Def Spec names it as chipboard.

		(Average 1.32cm^3/g)	
DEFSTAN 93-59	3.50 - 3.85 mm (Average 3.67 mm)	1.3 – 1.45 cm^3/g (Average 1.37 cm^3/g)	Min 2270 KPa (329 lb/sq in)

Currently, suppliers of strawboard are limited within the UK, with all suppliers acting only in a re-sale capacity and not producing the materials from a raw source. This is detrimental to any experimental campaign that requires increased quantities of fragment capture material. To provide an example, a test procedure can be found within the current ITOP (6) which includes the use of a Semi-Circular Fragmentation Arena. Using this procedure alongside the use of a 155 mm High Explosive (HE) shell, it is reported this test series would require in the region of 260 packs of strawboard (approximately £26,000 at the time of writing). Additionally, once perforated the strawboard sheets cannot be reused or recycled. Noting the importance, the target material has on understanding the dynamics of fragmentation, there is significant motivation to find cost effective alternatives which will help researchers better understand fragmentation interaction.

The aims of this work are therefore to classify the response of strawboard against a known fragment and impact velocities. This would allow for a comparison of uniform material response against two economical alternatives, resulting in a down selection to the most advantageous material. This would then be tested using high explosive charges to compare results from the previous gas gun experiments and provide a more granular analysis on the materials suitability for fragmentation capture.

2 Materials and Methods

2.1 Materials

Three target materials were investigated in this study: strawboard, MDF and underlay. Strawboard was supplied of dimensions 1000 mm x 800 mm x 3.5-3.85 mm and was used as the baseline, while MDF and underlay were identified as suitable replacements for strawboard due to their low cost, comparable dimensions, ready availability, and their conformity to relevant test standards. The MDF was supplied in panels measuring 2440 mm x 1220 mm x 4 mm,6 mm and 12 mm at a cost of £13.04, £17.34, £26.03 per panel and conformed to EN13986. The Fine Floor underlay was supplied in packs of 25 sheets where each sheet was 590 mm x 850 mm x 4 mm and cost £28.76 per pack and was selected due to its low cost and ease of availability.

Strawboard is currently procured in accordance with DEF STAN 93-59, is named as chipboard and made of good quality recycled paper. The bursting strength specified in the DEF STAN is measured using a Mullen Test apparatus. As the authors had no access to a Mullen Test apparatus, a three-point bend test using a Hounsfield universal testing machine was conducted to measure the ultimate tensile stress; the results are given in Table 2. Material orientation was not considered during testing due to lack of grain or directionality in the materials under test.

Whilst MDF is manufactured from pulped wood fibre, wax and a resin binder, the fibreboard underlay material consisted of wood chips, plant fibres, sawdust, cardboard, and paper and is 100% recyclable. This material has a proven track record of exhibiting high levels of compression strength and is traditionally used for hard flooring applications. As one of the prohibiting issues with the use

of strawboard is its availability, underlay was selected as a possible alternative. Underlay is readily available and provides soft capture options for fragmentation if this was an additional requirement.

Where required, layering of multiple thicknesses of the same material were used to reduce the overall witness capture pack thickness to a dimension suitable for the experiment in question as well as enabling a cost reduction.

Table 2 - Comparison of material thickness, grammage and experimentally determined Ultimate Tensile Stress (UTS)

Material	Thickness range (mm)	Grammage Range (cm³/g)	UTS (MPa)
Strawboard	3.5 - 3.85	1.3 – 1.45	8.50
MDF	4	1.39	59.67
MDF	6	1.39	59.67
MDF	12	1.39	59.67
Underlay	4	3.85	2.38

2.2 Gas Gun Projectile Configuration

To eliminate fragment orientation as a variable, a spherical 8 mm AISI 420, grade 100 stainless steel ball bearing of mass 2.1 g was used as an indicative fragment. For use within the gas gun the ball bearing was secured within a two-part 22 mm diameter acetal / polylactic acid (PLA) sabot and using a small quantity of plasticine. The complete fragment and sabot can be seen in Figure 1.
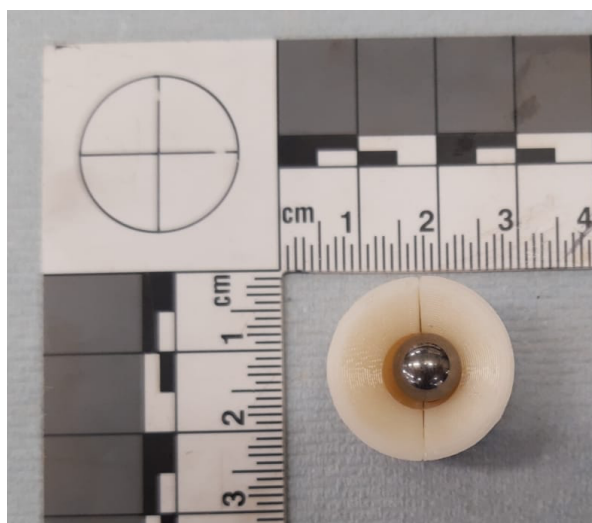

Figure 1 - Projectile and sabot set-up

2.3 Experimental Setup – Gas gun

A 22 mm bore Explosive Low Velocity Impact System (ELVIS) gas gun was used to deliver the projectile to the target material. These experiments were designed to investigate the energy absorption of these materials in a lower velocity regime. As these experiments were performed in the gas gun it allowed the study to be conducted in a laboratory setting as opposed to an explosive range. The gas gun included a sabot stripper to remove the sabot on exit from the muzzle which can be seen in Figure 2. The use of a gas gun allowed a rapid and repeatable method of accelerating the ball bearing to the required velocity. A diagram of the experimental set up is at Figure 3. The gas settings and indicative velocity achieved is in Table 3. The 'high' ballistic velocities indicated in Table 3 are indicative of ballistic velocities and not to be confused with explosively driven 'high' velocities which can easily reach 1000s of m s^{-1}. As fragment capture materials are used in both ballistic and explosive trials it is important to consider both 'high' velocity regimes. The high-speed camera used to measure the fragment velocity pre and post perforation of the target was a Phantom V12/12 high speed camera at 40,000 fps. The velocities were then measured using Phantom Camera Control (PPC) software v2.8. On perforation of the target (250 mm x 250 mm – Figure 2) the fragments were captured in a rag filled backstop which is integral to ELVIS. The fragments were not recovered for any further analysis. In all instances, both Strawboard and MDF target materials were repeatedly tested (n=4) for the MDF, whilst the Floor Underlay (n=2). This differed due to the low UTS result produced during the three-point bend test and analysis of data collected thus far.

Figure 2 - Target Set Up within the ELVIS Gas Gun target chamber and view of Sabot Stripper

Table 3 - Firing pressure and indicative velocities

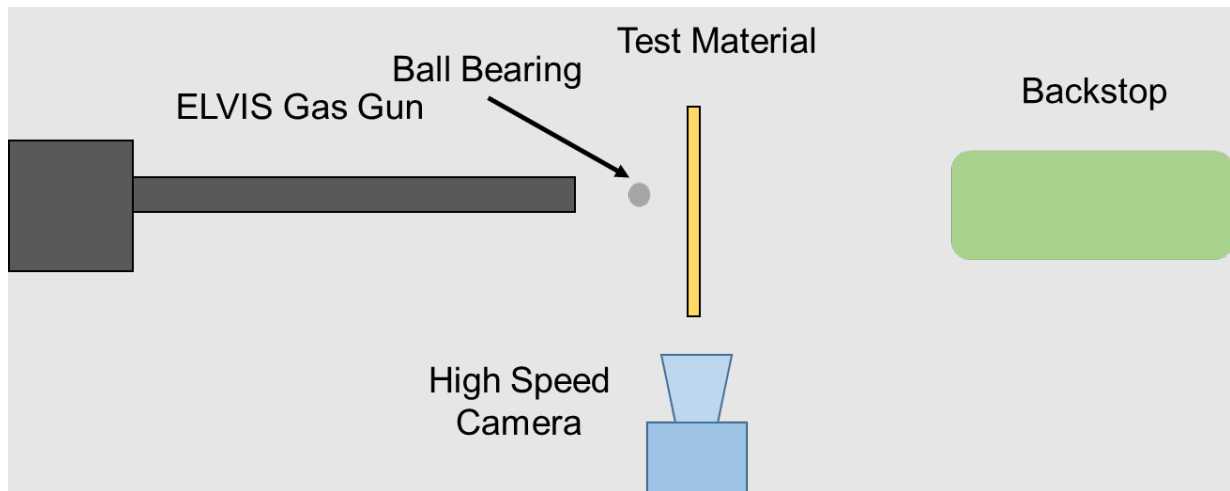| Velocity Range	Pressure (Bar)	Gas	Average Muzzle Velocity (ms^{-1})
Low	12	Air	257 ± 4.6
Medium	30	Air	365 ± 3.8
High	50	He^2	530 ± 14.9

**Figure 3 - Diagram of Experimental Set Up (Not to Scale)**

2.4 Explosive fragmentation charge design

Two fragmentation configurations, square and tessellated, were studied and selected to represent scenarios seen in the real world (39). In all studies, the explosive charge was rectangular in design, ensuring a symmetrical blast was created and additionally allowing for flat surfaces to attach the fragmentation packs (Figure 4). Samples were produced by tamping the explosive into a steel mould of dimensions 90 mm by 60 mm by 30 mm (Figure 5) to increase repeatability during charge manufacture. The charge used within this study was Plastic Explosive number 8 (PE8) and was selected due its malleability, insensitivity, and its availability. A Net Explosive Quantity (NEQ) of 100g was used to achieve a Velocity of Detonation (VoD) of ~8000 m/s (40). Explosive tamping was undertaken by a single individual to minimise variation amongst the charges.

Upon removal of the explosive from the mould, the ball bearings in either the square or tessellated configuration were placed on top of the pre-moulded explosive charge and secured using tape (Figure 5). The charge to mass ratio was 2:1 for a single layer of 8 mm ball bearings, 1:1 for two layers and 1:1.5 for three layers, and a packing density of 81% to 88% respectively. The packing density was calculated using the area covered by the ball bearings against the charge face size. This was done to reduce the edge effects that the rectangular charge would impart. Following attachment of the fragmentation and prior to detonation, the centre of each explosive was found, and a cavity for the detonator was established using a bore tool notched at a depth of 5 mm, thereby providing a frontal 25 mm of explosive. The detonators used were L2A2 electric detonators which were inserted to the rear of the charge. To further examine the effect of NEQ on material performance, PE8 quantities where also tested at 50 g and 200 g.

Figure 4 - Fragmentation Packing Lattice
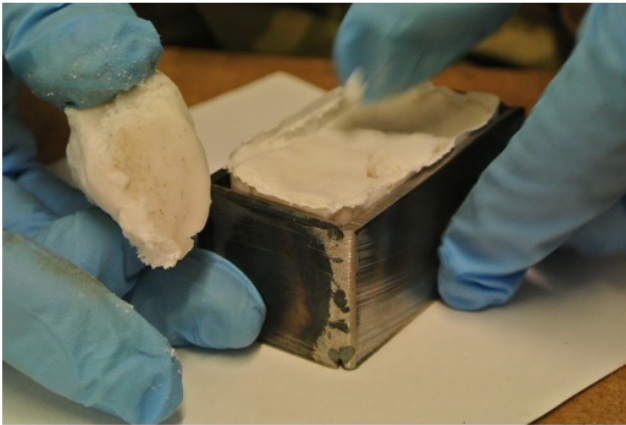
PE8 Moulding and Tamping
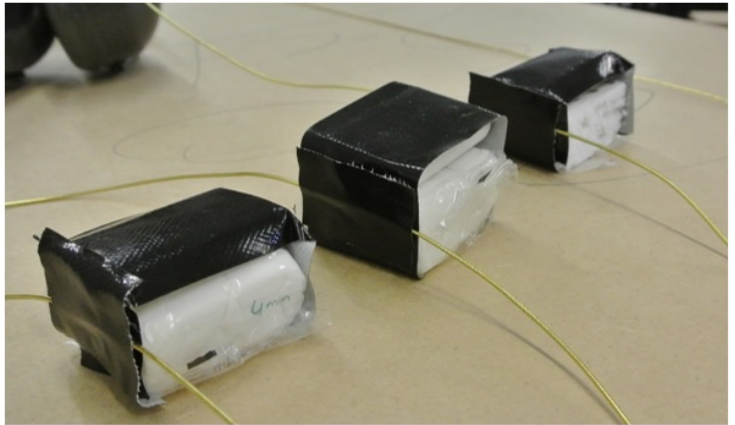
PE8 Charge Design

Figure 5 - Left: PE8 Moulding and Tamping. Right: PE8 Charge Design

2.5 Experimental Setup – Fragmenting Device

To assess the performance of the target materials, an explosive trial was performed. Prior to detonation, target materials were held in a fragment capture rig (Figure 6). The rig was designed and manufactured from mild steel box section and subsequently welded together to minimise damage and withstand the explosive blast. The explosive charge was placed on top of the initiation platform which was located 1 m from the first MDF board after a trial of 2 m was examined and determined to not give a suitable fragmentation pattern to generate data. Tests were conducted within a containment building located on the Explosives Research Detonation Area at the Defence Academy Shrivenham site. The majority of the experimental trials were conducted using a spaced fragment capture system and one unspaced. This was to enable the mass of the system to be reduced to make it a more attractive alternative capture material and the unspaced system was used to provide a baseline for previous trials and future work. This is discussed in further detail in the discussion section.

Figure 6 - Test Set Up / Rig Design

For each firing, the number and position of the fragments that hit the MDF panels were recorded and tabulated using cartesian coordinates starting from the centre of the panel. Data was then imported to MATLAB 2018 software, where replication of the fragmentation pattern was created using graphical representations and used to compare the differing distributions and fragment trajectories between target arrangements. To provide further evidence for repeatability and reliability of the material being interrogated.

3 Results

3.1 Quantification of ballistic residual velocities

Figure 7 shows the relationship between the recorded strike velocity and the residual velocity for all three materials where the strike velocity was shown to be independent of the velocity lost by perforation of the material. This effect is highly reproducible as the R^2 is 0.99 for all three data sets, where the relationship between the three materials is linear, so an equivalence between the different materials can be identified. This is crucial to understand how energy is lost in the proposed capture materials to enable alternatives to be quantitatively characterised. The results and standard deviations are provided in Table 4 where the data shows that the high velocity series for all materials resulted in increased deviation across all results and as such this data will be disregarded for the rest of the study (identifiable by *). The higher velocity energy absorption will be characterised in the second test series using explosive charges.
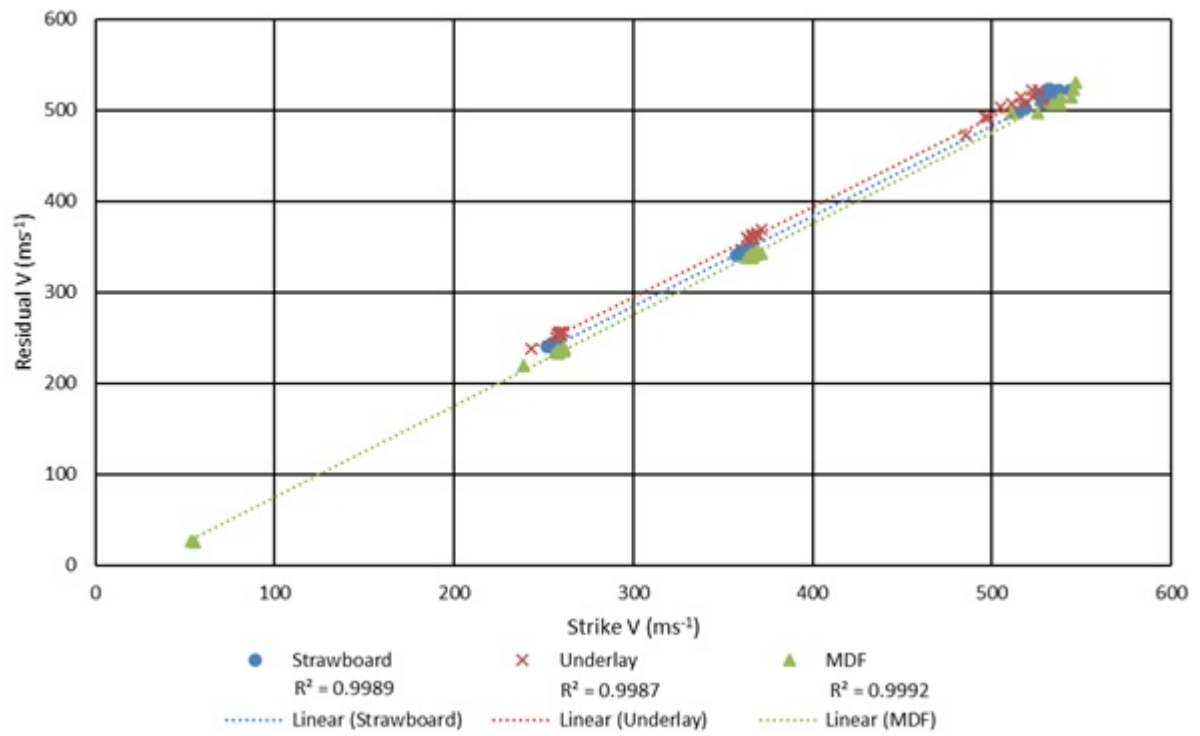
Figure 7 - Graph of strike velocity vs residual velocity of 3.5-3.85 mm thick strawboard, 4mm thick MDF and 4 mm thick underlay

Table 4 - Mean velocity loss recorded for each tested materials at low, medium, and high velocity impacts (average muzzle velocities defined in Table 3)

Material	Mean Velocity Loss (ms⁻¹)	Standard Deviation (ms⁻¹)	SD as a percentage of Mean
Low Velocity			
3.6 mm Strawboard	14.22	2.07	15%
4mm Underlay	4.6	1.01	22%
4mm MDF	23.19	1.81	8%
Medium Velocity			
3.6 mm Strawboard	17.16	2.08	12%
4mm Underlay	4.96	1.69	34%
4mm MDF	24.95	2.4	10%
High Velocity*			
3.6 mm Strawboard	17.34*	6.4*	37%*
4mm Underlay	7.47*	6.51*	87%*
4mm MDF	25.38*	5.62*	22%*

Table 5 - Mean velocity loss recorded for different sheets tested of strawboard, underlay and MDF

Sheet Number	Mean Velocity Loss as a percentage of Impact Velocity (%)	SD
Strawboard		
Sheet 1	4.64	0.89
Sheet 2	4.74	1.29
Sheet 3	4.2	1.6
Mean	***4.53***	***1.27***
Underlay (4 mm Thick)		
Sheet 1	8.34	7.25
Sheet 2	4.97	3.8
Sheet 3	4.64	2.22
Sheet 4	4.79	1.27
Sheet 5	4.96	3.41

Sheet 6	5.96	3.95
Mean	*5.61*	*3.65*

<div align="center">

MDF (4 mm Thick)

</div>

Sheet 1	24.28	7.28
Sheet 2	24.41	4.77
Sheet 3	24.74	3.73
Mean	*24.47*	*5.26*

The strawboard sheets were made by the same manufacturer to a known standard, so it was expected that the response (velocity loss through energy absorption) should be uniform. This is not the case as demonstrated by the values in Table 5 where the standard deviation varies between sheets. This is far from what would be expected for a known and extant standard.

The comparison of the six sheets of the underlay shows a greater variance in response compared to strawboard. This is because as the velocity lost by perforation is very small, a very small deviation can result in a very large percentage error. Variance of response of the MDF is apparent between the three sheets, even though the three sheets were cut from the same panel. This range of response is lower than the other two materials. MDF has the advantage of a high mean value which reduces the impact of the standard deviation. The MDF shows greater uniformity between sheets than the strawboard and underlay. The underlay shows extremely poor uniformity between sheets and has the worst percentage SD of the Mean and as such was not used further in this study. Alternatively, based on the quantitative results demonstrated in this test series, MDF was taken forward for explosive testing as the most promising alternative candidate material to strawboard.

3.2 Penetration Capacity of explosively driven projectiles

Verification of the results shown within 3.1 were conducted using a series of 50 g, 100 g and 200g charges of PE8 against a strawboard pack containing strawboard sheets of a supplied thickness of 3.65 mm. In all instances the ball bearings perforated the material, splintering the rear of each panel with minimal interaction within the strawboard pack. As one of the principal roles of strawboard is to record fragmentation patterns from materials failure induced by explosive events this is not considered an experimental failure.

With the results from gas gun trials showing promise for the MDF material, the second stage of the experiment was broken down into six bespoke areas focussing on single, double, and triple layer configurations, fragmentation interaction, witness screen separation distance and an evaluation of charge scaling effects (Table 6). These configurations were selected to replicate common experimental set up used in commercial/academic trials (41).

Table 6 - High Explosive Experimentation Results – MDF (NEQ - Net Explosive Quantity)

								High Explosive Experimentation Results - MDF
Serial No.	NEQ Used (g)	Distance from Target (m)	No. of Ballbearings	Sheet Thickness (mm)	Distance Between Sheets (mm)	No. of Sheets	Fragments on Target	Max Depth of Pentration
1	100	1	25 - Single Layer	6	100	12	22	Perforation (Sheet 12)
2	100	1	25 - Single Layer	6	100	12	22	Perforation (Sheet 12)
3	100	1	25 - Single Layer	4 x 6 / 5 x 12	100	9	25	Perforation (Sheet 12)
4	100	1	25 - Single Layer	12	100	12	10	Sheet 8
5	100	1	25 - Single Layer	12	100	12	10	Sheet 8
6	100	1	50 - Double Layer	3 x 6 / 7 x 12	100	10	15	Sheet 6
7	100	1	75 - Triple Layer	3 x 6 / 7 x 12	100	10	11	Sheet 6
8	100	1	50 - Double Layer	6	0	20	10	Sheet 12
9	200	1	50 - Double Layer	11 x 12 / 1 x 18	100	12	19	Sheet 7
10	200	1	50 - Double Layer	11 x 12 / 1 x 18	100	12	20	Sheet 6
11	50	0.5	50 - Double Layer	7 x 12	100	7	22	Sheet 5
12	50	0.5	50 - Double Layer	2 x 12 / 8 x 6	100	10	11	Sheet 5

To determine the optimal capture configuration of both the thickness, order, and number of MDF sheets several serials were conducted (Table 6). Serial 1 utilised the full target rig capacity of 12 panels at 6 mm thick, paired with a 100 g PE8 explosive charge which had a single layer of 25 ball bearings. The initial qualitive assessment indicated a good fragment distribution pattern, where 90% of the ball bearings were captured within the MDF target arrangement. Perforation was apparent throughout all 12 panels which indicated a target overmatch which was confirmed by a repeat experiment. This can be seen in Figure 9, thus, subsequent experiments used 12 mm thick MDF sheets.

Serial 1 was repeated with four 6 mm panels located in front of five 12 mm panels. This resulted in 12 of the 25 ball bearings penetrating all nine MDF boards with enough energy to impact the wall of the containment building. This was repeated with a full complement of 12 mm MDF sheets with results showing that 10 of the 25 ball bearings had hit the target material with 2 ball bearings stopping after 9 MDF panels and 3 stopping after 8. This was repeated, with outcomes showing the same results.

An additional layer of ball bearings was used to create a double layer. This was detonated against three 6 mm panels which were located in front of seven 12 mm MDF panels. This resulted in 15 of the 25 ball bearings hitting the target, 3 stopping after 6 panels, 6 after 5 and 3 after only 3 panels.

Serial 7 focussed on adding a further layer of fragmentation (75 ball bearings) to explore whether an increased number of fragments used had any effect on MDF's ability to accurately record depth of penetration. The number of MDF panels remained the same, which resulted in two ball bearings stopping after two panels, seven after five and two after five. The 6mm front sheet of MDF can be seen in Figure 8. A total of 64 ball bearings missed the target, this is predicted to be due to a significant increase of fragmentation interaction during expulsion from the charge.

Figure 8 – 6 mm thick MDF front sheet post exposure to a 100 g charge of PE8 containing 75 ball bearings at 1 m range.

Once the results had been gathered and the thickness, order, and number of MDF sheets were optimised, it was decided to explore the effect that spacing of the MDF sheets may have on the projectiles ability to perforate the material, based on spaced armour principles (42). The experimentation with MDF sheets in this spaced configuration versus those that had 0mm spacing between them was negligible and therefore was a result of note in this study.

For serial 8 an examination on twenty 6 mm MDF sheets were used to assess whether spacing between the target materials has any effect on its ability to perform advantageously. 50 ball bearings in a double layered configuration were used to increase the hit probability. The other parameters remained unchanged. It was found that only 10 hits were on target, accounting for less than 20% of the total bearings loaded to the charge. Penetration had occurred through a maximum of 12 layers of MDF. It was concluded that penetration capability is in line with the previous serials and that the configuration of MDF panels does not affect the bearings velocity and energy available for penetration, however further investigations are required to clarify this work.

To further explore the effect of charge mass (increase in potential energy/velocity) and thus the potential of MDF as an alternative capture material, the NEQ was increased to 200 g to evaluate dispersive and penetrative fragmentation. The first MDF sheet was 18 mm thick to provide greater resilience against the enhanced blast from the higher NEQ, whilst the subsequent 11 MDF sheets remained at 12mm thickness. A double layer of 8 mm ball bearings formed the fragmentation. Analysis after firing showed 11 ball bearings embedded within sheet 5, with a further 8 having stopped in sheet 7. Accounting for the increased resistance of the initial 18 mm MDF board, as well as the developing trend between multi-layered fragmentation and lessened penetration, for the double layered ball bearings to have penetrated as many sheets as single layered firings reinforced the correlation between greater NEQs and enhanced fragment velocities and penetration. However, full validation of this was inhibited by the damage inflicted upon the first 4 MDF sheets, leaving only the final 8 sheets to contrast with firings of lesser NEQs. When compared with the strawboard targets there was not a significant difference in the damage inflicted on the front face of the 2

materials. This was repeated, with the results showing 7 ball bearings embedded within sheet 5 and a further 13 in sheet 6.

The charge size was then decreased to 50 g and positioned closer to the target (Table 6) to investigate the response to a lower charge size as well as change in fragment distribution pattern. A PE8 charge of 50 g was placed 50 cm from the first of seven 12 mm MDF sheets (total thickness 84mm). A double layer of 8 mm ball bearings was used to form the fragmentation. Analysis after firing showed 5 ball bearings embedded in sheet 3, 9 in sheet 4, and 8 in sheet 5. This was repeated to test the authenticity of the results obtained. The only difference in test set up was in the configuration of the MDF, where the first 2 sheets were comprised of 12 mm boards, followed by 8 boards of 6 mm MDF (total thickness 72mm). This alteration was due purely to resource availability by this late stage in testing. Analysis after firing showed 6 ball bearings embedded in sheet 5, 4 in sheet 6 and 1 in sheet 7. After factoring in the reduced MDF thickness from this firing, contrasting the combined results from serials 11 & 12 with those from serials 2 & 3 (where identical test configurations were used but with a greater NEQ) implies the expected correlation between lower NEQs and subsequently reduced fragment velocities and penetration in the target material.

To further analyse the results, cartesian coordinates were captured from the target materials and used to create a graphical representation to show the direction of travel of the ball bearings. During examination of fragmentation laid out in a single layer configuration, it was found that the fragmentation distributions show an average of 20 fragment hits per square meter. This is shown in Figure 9.
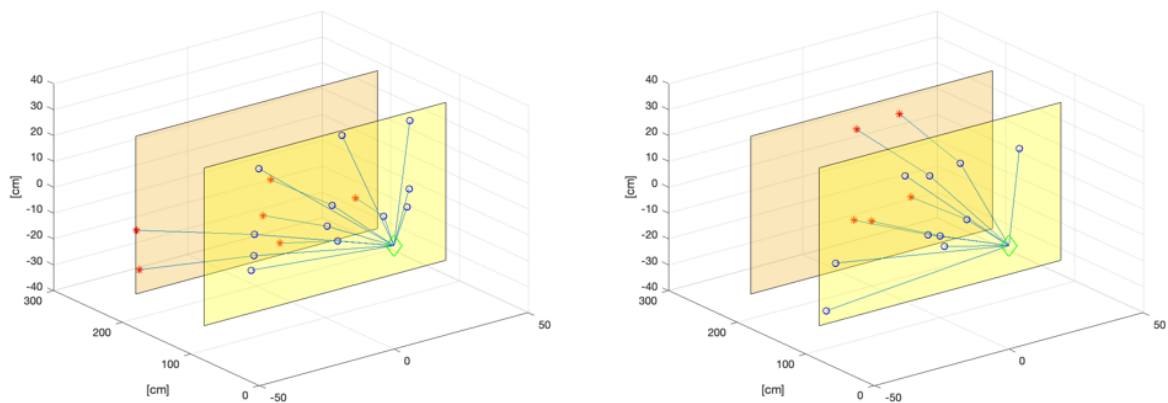

Figure 9 – Left: Serial 1 and Right: Serial 2 - MDF fragment distribution pattern for 1-Layer of ball bearings fired from 100 g PE8 charge at 1 m range.

Another parameter considered was the charge mass and its influence on the fragment distribution on the target. Charges of 50 g, 100 g and 200 g were fired in the same conditions and with the same number of fragment layers and the respective results are shown below in Figure 10.
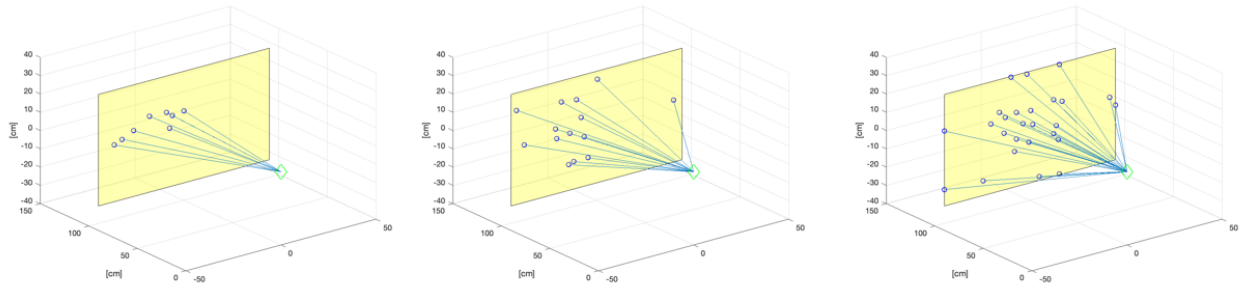
Figure 10 - Fragment Distributions for Left: Serial 11 (50 g), Middle: Serial 6 (100 g) and Right: Serial 10 (200 g)

4 Discussion

Of the alternative materials suggested (MDF and underlay) MDF emerged as the most promising alternative candidate. Underlay whilst readily available, cheap and its adherence to certain standards gave it validity as a fragment capture alternative, particularly when procurement issues with strawboard is one of the major drivers in researching an alternative. Its energy absorption properties and UTS values especially considering the standard deviations calculated for the results demonstrate its inability to be considered a viable alternative. Underlay was proven to have the poorest uniformity between sheets, the largest percentage error when calculating the strike velocity and is the most expensive material when its equivalence to strawboard is considered. These facts alone do not necessarily negate its use as a fragment capture material. It has proven to have the lowest limiting velocity of the three tested materials and thus it would still be able to provide data on fragmentation which would be unable to perforate a strawboard witness pack. This may have applications where fragmentation data needs to be collected from slow moving fragments, such as the testing of non-lethal systems. The reduced unit price means that underlay is also a very suitable material for use as a witness board when the only data required to be collected is the fragmentation dispersion pattern.

The strawboards performance in this study demonstrated that the value of the measured limiting velocity for steel fragments is not the same as that recorded by McMahon (37) and the value of K (see Equation 1) in McMahons equation for spherical fragments is essentially a factor of 2 different to that which has been measured. If we calculate the strike velocity for this experiment using McMahons value for K, then this gives a result of 308 ms^{-1}, whereas in this study the strike velocity was recorded as 261 ms^{-1}. The use of McMahons value of K will result in an over estimation of strike velocity by 20%. There are three possible explanations for this; 1) this experiment was only completed once for strawboard, so this could be an outlying result, 2) that the currently available strawboard material is now significantly different to that used by McMahon, and 3) There is an inconsistency in McMahon's calculated values for K and V_L (see Equation 1). There is a limited data set to prove that the McMahon values are inconsistent, only that the results reported herein deviate from the original work. These figures deviate by a measured 7% difference in V_L that was observed between the two figures and the values of K are different by a factor of 2.

Comparison of the DEF Spec 81/001 (16) and the DEFSTAN 93/59 (26) does show that there is a difference, albeit very small, in the standard against which strawboard is currently manufactured versus the strawboard manufactured in the 1960s-70s. It is therefore possible that the current strawboard and the strawboard used by McMahon in the 1970s may not be the same material or

have the same properties. However, there is no known supply of strawboard from the 1960s available to prove these assertions.

We can take the results presented within this study utilising the original strike velocity from the McMahon fragment penetration equations (37), which now can be modified for an alternative fragment capture material. This led to an aim of identification of the required constants which are unique to each fragment capture material.

$$V_S = \frac{KP}{M^{\frac{1}{3}}\rho^{\frac{2}{3}}} + V_L$$

<div align="right">**Equation 1**</div>

V_s is the Strike Velocity (ms^{-1}).

K is the constant for a given fragment shape and fragment capture material.

P is the penetration depth (mm).

M is the mass of the fragment (mg).

ρ is the density of the fragment (gm/cm^3)

V_L – Limiting velocity (ms^{-1})

Equation 1 is independent of the fragment material as this is considered by the $1/\rho^{2/3}$ element. There are two derived values, which are the constant for a given fragment shape (K), and the lower cut off velocity (V_L). In McMahon, the value of K is given as 337 for spherical fragments (37). This constant is only suitable for use when strawboard is the capture material. The second derived value is the lower cut off velocity (V_L), which is the velocity at which the fragment does not penetrate further into a witness pack. McMahon gives the value of V_L as 205 ms^{-1} (37) for strawboard. Both constants are derived values which are suitable for use with any fragment material. To derive a conversion method for different fragment capture materials, both constants must be calculated. The V_L can be ascertained by experimentation, while K can be found by making K the subject of Equation 1 to give:

$$K = \left(\frac{(V_S - V_L)M^{\frac{1}{3}}\rho^{\frac{2}{3}}}{P} \right)$$

<div align="right">**Equation 2**</div>

The limiting velocity (V_L) was experimentally determined by calculating the average velocity reduction of the fragment of a single sheet (V_B) of each material following perforation. As the velocity lost by perforation of a single sheet is known, the value of V_L was found by keeping the same experimental setup throughout but utilising a witness pack of sufficient thickness to capture the fragment. The thickness of the overmatched witness pack was taken as 10 layers of strawboard; this was from an estimated penetration depth of two sheets that was then multiplied by five. As the MDF was a stronger material than the strawboard, the overmatched witness pack could be thinner; as such eight layers of MDF were used.

The thickness of the underlay pack was more difficult to estimate, as the V_L was expected to be in the 50 - 60 ms^{-1} region, and a witness pack of this size was too thick to fit into the apparatus. To reduce the thickness of the underlay pack to a workable size the first three layers were strawboard, with the remainder being 30 layers underlay. It was known that the fragment would penetrate three layers of strawboard, while the 30 layers of underlay proved to be sufficient to capture the

fragment. The penetration depth of the fragment in sheets was then measured and used to calculate the V_L using Equation 3.

$$V_L = V_S - (P \times V_B)$$

<div align="right">**Equation 3**</div>

Once the depth of penetration of the captured fragment in the witness pack had been measured, and the V_L was calculated, Equation 2 was used to give a value of K for spherical fragments into that capture material (Table 7). The value for strawboard V_L matches the value given by McMahon for the average V_L across all fragment materials. The experimental value of V_L specifically for steel fragments is 190 ms^{-1} (37). The value of K calculated (Table 7) is significantly different to the 337 that is quoted in McMahon (37).

Table 7 - Calculation of Limiting Velocity (V_L) and constant (K) for strawboard, MDF and underlay

Serial	Material	Penetration (layers)	V_S (ms^{-1})	V_L (ms^{-1})	V lost by perforation (ms^{-1})	K
1	Strawboard	4	261	204	56.8	179
2	MDF	2	261	217	44	277
3	Underlay	20	260	167	93.2	58

In Equation 1 the term given to describe different fragment materials is $1/\rho^{2/3}$. This also required that a single value of V_L and K be calculated. McMahon determined the V_L by plotting penetration depth against strike velocity for each fragment material, and the equation of this linear relationship gives the value of V_L for that material. The value of V_L for Equation 1 was the mean of the V_L across 5 fragment materials, as this mean then had a standard error of 9.2 this was taken as suitable for the equation.

The identification of the K value was found by McMahon by plotting of the $Log_{10}K$ against the $Log_{10}\rho$ for each fragment material enabling a linear regression line. The equation of the resulting regression line then gives the value of K for spherical fragments as 337. This was completed for face on impact of cubes, and irregular fragments in the same way. As this work was completed in 1970, there is the possibility that the measured velocities and computation of results may be the cause of this difference in K value (Table 7), due to present day improvements in experimental methodologies and techniques.

While the suitability of MDF was clearly demonstrated by ballistic trails utilising gas guns and as demonstrated the mathematics holds, the main requirement of an alternative capture material for strawboard is the use of this in explosive fragmenting trials. The equations governing behaviour in a non-ideal laboratory environment e.g., an outdoor explosive range require additional terms in the equation.

 The main objective for the MDF material is to measure the depth of penetration of the fragment and therefore energy absorption of the target material. This should be conducted by establishing the penetration values fragments achieved in to the MDF, which allows for calculation for the initial velocity (V_s). This would be calculated by substituting this velocity into Equation 4 and solving for the range (S). This is a common parameter required for analysis when using explosive charges and is

derived from the balance between air drag and inertia deceleration. The value used for air drag coefficient (C_d) being 0.47 (43) with the assumption being the ball bearings will maintain the shape of a sphere. Other parameters used are air density (ρair) of 1.225 kg/m^3, fragment mass (m) of 2.09 g, cross section area (A) for a spherical ball bearing of diameter 8 mm (See Appendix I for calculation details).

$$V_{crit} = V_s \exp\left[-C_d \rho_{air} S\left(\frac{A}{2m}\right)\right]$$

Equation 4

Where: V_s = the initial velocity

S = range

C_d = air drag co-efficient

ρair – Density of air

m = fragment mass

A = cross sectional area

The initial approach to evaluate the initial velocity was to employ the McMahon equation as used in the previous gas gun trials. However, having applied this method to the results gathered within the high explosive trials, it was apparent the values of V_s were greater than expected by a factor varying between four and seven, leading to the re-evaluation of the witness screen material thickness.

Various thicknesses of MDF were tested in the spaced fragment capture arrangement and showed that 6 mm MDF is not suitable for trials involving 100 g of PE8. The resultant shockwave, coupled by the blast from the explosive charge is thought to have played a part in weakening the structural integrity of the first panel, whilst the remaining panels were simply overmatched by the velocity of the projectiles. This was not verified with subsequent mechanical testing due to time constraints but should be validated in further work to confirm the assumption. 12 mm thick MDF has been proven to be most advantageous when testing 50-100 g of PE8 due to its mass, whilst an initial panel of 18 mm thick MDF would be required for NEQ's between 100 and 200 g. This has shown to be for the same reasons the initial 6mm panels were overmatched during the first two high explosive serials. Whilst this investigation of how explosive charge size affects MDF thickness has been shown to have utility with increasing quantities of explosive, to ensure the fragment capture set up uses as less mass as possible to increase the sustainability element of the research a spaced capture set up was utilised. It is also noted that this creates an additional variable in the experimental set up which is often not ideal. Therefore, further works needs to be conducted to provide additional data to the that presented within this paper.

Conclusions

In this study an economic alternative to strawboard has been identified for fragmentation testing. The initial experimental data set demonstrated the equivalence between three materials selected for assessment of target energy absorption from a spherical fragment. It was found during

comparison of the three materials that MDF was not only 25% cheaper than the traditional Strawboard material but performed better in both Gas Gun (ballistic) data and explosive testing scenarios.

The ability for MDF to be produced to a set industry standard lends itself to repeatability which should be placed at the forefront of any research, allowing for experiments to be reproduced, but also lowering the risk of inconstancies between batches of material.

It was proven that the McMahon equation could be modified for a different witness material and the values of K and V_L were derived for both MDF and underlay. This allowed the identification of an equivalence between fragment capture materials so that they can be equated and interchanged. This is caveated to 8 mm ball bearings within this study. Ultimately demonstrating that a cheaper, more readily available material – MDF, can be and arguably should replace the current industry standard fragment capture material - strawboard.

5 Acknowledgements

6 Funding

7 Conflicts of Interest

The authors declare no conflict of interest.

8 References

1. Critchley R, Hazael R, Bhatti K, Wood D, Peare A, Johnson S & Temple T (2022) Blast mitigation using polymeric 3D printed auxetic lattice structures - a preliminary study, International Journal of Protective Structures, 13 (3) 469-486.

2. Thawani B, Hazael R & Critchley R (2021) Numerical modelling study of a modified sandbag system for ballistic protection, Journal of Computational Science, 53 (July) Article No. 101403.

3. Bloodworth-Race S, Critchley R, Peare A, Hazael R & Temple T (2021) Testing the blast response of foam inserts for helmets, Heliyon, 7 (5) Article No. e06990.

4. Rao P, Painter J, Appleby-Thomas G, Critchley R, Wood D, Roberts & Hazael R (2020) Fragmentation studies by non-explosive cylinder expansion technique, International Journal of Impact Engineering, 146 (December) Article No. 103714.

5. Reynolds M, Huntungton-Thresher W. 2016. "Development of tuneable effects warheads," Defence Technology, vol. 12, pp. 255-262,

6. United States Army (US Army) Test and Evaluation Command, 30 Mar 1993. "International Test Operations Procedure 4-2-813," Aberdeen Proving Ground.

7. Gold M, 2017. Fragmentation model for large L/D (Length over Diameter) explosive fragmentation warheads, Def. Technol. 13 2017 300–309. doi:10.1016/j.dt.2017.05.007

8. da Silva L.A, Johnson S, Critchley R, Clements J, Norris K, Stennett C, 2020. Experimental fragmentation of pipe bombs with varying case thickness, Forensic Science International, 306 (January) Article No. 110034

9. Arnold W, Rottenkolber E, 2008. Fragment mass distribution of metal cased explosive charges, Int. J. Impact Eng. 35 1393–1398. doi:10.1016/j.ijimpeng.2008.07.049

10. Grady D.E, Kipp M.E. (1985) Mechanisms of dynamic fragmentation: factors governing fragment size, Mech. Mater. 4 (3e4) 311e320

11. Mott N.F, 1947. Fragmentation of shell cases, Proc. R. Soc. A Math. Phys. Eng. Sci. 189 300–308. doi:10.1098/rspa.1947.0042.

12. Ugrčić M, Ivanišević M, 2015. Characterization of the Natural Fragmentation of Explosive Ordnance Using the Numerical Techniques Based on the FEM, Sci. Tech. Rev. 65 14–27. doi:10.5937/STR1504016U

13. Goloveshkin V.A, Myagkov N.N, 2014. Fragmentation model for expanding cylinder. Int J Fract 2014;187:239–43.

14. Breeze J, Leason J, Gibb I, Allanson-Bailey L, Hunt N, Hepper A, Spencer P, Clasper J, 2013. Characterisation of explosive fragments injuring the neck. Br J Oral Maxillofac Surg. 2013;51(8):e263–6.

15. Ugrčić M, 2013. Numerical Simulation of the Fragmentation Process of High Explosive Projectiles, Sci. Tech. Rev. 63 (2013) 47–57. http://www.vti.mod.gov.rs/ntp/rad2013/2-13/3/3.pdf.

16. Ministry of Defence Defence (MOD) Logistics Organisation, 2017. "Defence Standard 81 - 148 Board, Processed Wood for general packaging," MOD, 2017.

17. Ren G.W, Guo Z.L, Fan C, Tang T.G, Hu H.B, 2016. Dynamic shear fracture of an explosively-driven metal cylindrical shell. Int. J Impact Eng 2016; 95:35-9.

18. Moxnes J.F, Prytz A.K, Frøyland Ø, Klokkehaug S, Skriudalen S, Friis E, Teland J.A, Dørum C, Ødegårdstuen G, 2014. Experimental and numerical study of the fragmentation of expanding warhead casings by using different numerical codes and solution techniques. Def Technol 2014;10:161-76

19. Gregory O, Oxley J, Smith J, Platek M, Ghonem H, Bernier E, Downey M, Cumminskey C, 2010. Microstructural characterization of pipe bomb fragments, Mater. Charact. 61 (2010) 347–354. doi:10.1016/j.matchar.2009.12.017

20. Vogler T.J, Thornhill T.F, Reinhart W.D, Chhabildas L.C, Grady D.E, Wilson L.T, 2003. Fragmentation of materials in expanding tube experiments. Int J Impact Eng 2003; 29:735–46.

21. Stronge W.J, Ma X.Q, Zhao L.T, 1989. Fragmentation of explosively expanded steel cylinders. J Mech Sci 1989;31:811-23

22. Ministry of Defence (MOD), 1961. "Defence Specification 81-001," Her Majesty's Stationary Office, London, 1961

23. Gullerud A, Hollenshead J, 2017. Coupled Euler-Lagrange simulations of metal fragmentation in pipe bomb configurations, Procedia Eng. 204 (2017) 202–207. doi:10.1016/j.proeng.2017.09.774

24. Grisaro H, Dancygier A.N, 2015. Numerical study of velocity distribution of fragments caused by explosion of a cylindrical cased charge, Int. J. Impact Eng. 86 (2015) 1–12. doi:10.1016/j.ijimpeng.2015.06.024.

25. Bors D, Cummins J, Goodpaster J, 2014. The Anatomy of a Pipe Bomb Explosion: Measuring the Mass and Velocity Distributions of Container Fragments, J. Forensic Sci. 59 (2014) 42–51. doi:10.1111/1556-4029.12294

26. Ministry of Defence Defence (MOD) Logistics Organisation, 2005. "Defence Standard 93-59 Chipboard (For use at Proof and Experimental Establishments)," MOD, 23 September 2005.

27. Gurney W. 1943. The initial velocities of fragments from bombs, shell and grenades, Report No. 405. Dayton: Ballistic Research Laboratories; 1943.Google Scholar

28. Ministry of Defence, Defence Logistics Organisation, 2003. "Defence Standard 13-184 Millboard and Millboard, Leadfree," MOD, 19 Dec 2003

29. Grady D.E, Benson D.A, 1983. Fragmentation of metal rings by electromagnetic loading. Exp Mech 1983;23:393–400

30. Li Y, hua Li Y, quan Wen Y, 2017. Radial distribution of fragment velocity of asymmetrically initiated warhead, Int. J. Impact Eng. 99 (2017) 39–47. doi:10.1016/j.ijimpeng.2016.09.007.

31. Huang G.Y, Li W, Feng S.S, 2015. Axial distribution of Fragment Velocities from cylindrical casing under explosive loading, Int. J. Impact Eng. 76 (2015) 20–27. doi:10.1016/j.ijimpeng.2014.08.007.

32. Cullis I.G, Dunsmore P, Harrison A, Lewtas I, Townsley R, 2014. Numerical simulation of the natural fragmentation of explosively loaded thick walled cylinders, Def. Technol. 10 (2014) 198–210. doi:10.1016/j.dt.2014.06.003

33. AL-Hassani S.T.S, Hopkins H.G, Johnson W, 1969. A Note on the fragmentation of tubular bombs. Int J Mech Sci 1969;11:545e9

34. Gold V.M, Baker E.L, 2008. A model for fracture of explosively driven metal shells. Eng Fract Mech 2008;75:275-89

35. Read J, Hazael R, Critchley R. Soft Tissue Simulants for Survivability Assessment; A Sustainability Focussed Review. Applied Sciences 2022, Vol 12, Page 4954 [Internet]. 2022 May 13; 12(10):4954. Available from: https://www.mdpi.com/2076-3417/12/10/4954/htm

36. Oxley J.C, Smith J.L, Bernier E.T, Sandstrom F, Weiss G.G, Recht G.W, Schatzer D, 2018. Characterizing the Performance of Pipe Bombs, J. Forensic Sci. 63 (2018) 86–101. doi:10.1111/1556-4029.13524

37. McMahon G.E, 1971. "The relationship between velocity of impact and the penetration into strawboard of fragments of different densities," RARDE, 26 Nov 1971.

38. Flynn D.J and Battenbo H, 2017. "Method and apparatus for characterising fragmentation of an explosive device". The United Kingdom of Great Britain and Northern Ireland Patent 1316508.9, 17 September 2017

39. US Department of Homeland Security. IED Attack – Improvised Explosive Devices. Available at: IED Attack: Improvised Explosive Devices (dhs.gov)

40. Chemring Energetics UK, 2016. PE8 Plastic Explosive. 2016; (1): 18001. Available at: https://www.chemring.com/~/media/Files/C/Chemring-V3/documents/energetics/PE8%20Plastic%20Explosive%20Iss%2013%20Nov%2020.pdf

41. Williams MGG., Turner GR., Lee M., Smith BD., Carr DJ., Malbon C., et al. Performance of police personal protective equipment challenged with a military grenade. https://doi.org/10.1177/0032258X18785859. SAGE Publications Sage UK: London, England; 16 August 2018; 92(3): 191–202. Available at: DOI:10.1177/0032258X18785859

42. I.Horsfall, E.Petrou, S.M.Champion. SHAPED CHARGE ATTACK OF SPACED AND COMPOSITE ARMOUR. In: 23rd International Symposium on Ballistics. TARRAGONA, SPAIN; 2007. p. 8.

43. Hoerner S.F, 1965. Fluid-Dynamic Drag. 1965 [3rd]. 1965. Available at: http://ftp.demec.ufpr.br/disciplinas/TM240/Marchi/Bibliografia/Hoerner.pdf

9 Appendices

Appendices 1 – Derivation of Fragmentation Velocity Decrease Equation

$$V_{crit} = V_s \exp\left[-C_d \rho_{air} S\left(\frac{A}{2m}\right)\right]$$

The velocity of a travelling fragment can be expressed as a function of the distance from the starting location, knowing its starting velocity and physical characteristics. To do so, we consider the resistance exerted by the air to be the main mechanism by which the fragment slows down, while gravity is considered a second order effect for most of the flight and therefore its contribution assumed to be negligible. In the proposed scenario, air drag is balanced by inertial deceleration, both expressed in terms of force.

Fragment deceleration can simply be expressed in terms of mass and acceleration, and then substituting for a general fragment of area A, height h and density ρ_m: (Note[2])

$$F = ma = (Ah\rho_m)\frac{dv}{dt}$$

while the drag equation derives from a definition of force as a function of pressure and area, where the pressure is then expressed with Bernoulli equation for a moving fluid. The drag coefficient C_d is a factor that considers other variables, such as shape, texture and viscosity that can influence the drag.

$$D = PA = C_d\left(\frac{1}{2}\rho_{air}v^2\right)A$$

Balancing the drag with the inertia deceleration gives:

$$(Ah\rho_m)\frac{dv}{dt} = C_d\left(\frac{1}{2}\rho_{air}v^2\right)A$$

---

[2] formula can be subsituted where necessary for different fragment geometries.

Which can be written as:

$$L\frac{dv}{dt} + v^2 = 0$$

Where the characteristic length L is expressed by

$$L = \frac{h\rho_m}{\frac{1}{2}\rho_{air}C_d} = \frac{m/A}{\frac{1}{2}\rho_{air}C_d}$$

The solution to the first-order differential equation gives:

$$v = v_o e^{-x/L} = v_o e^{-\rho_{air}C_d(\frac{A}{2m})x}$$

with v_0 initial velocity, v terminal velocity and x the distance reached by the fragment.